Journal of Functional Materials and Applied Engineering

Research Paper

Highly Efficient KOH Activation Method for the Formation of Enzymatic Hydrolysis Residual Lignin-Based Porous Carbon Materials

Jerzy Alshareef[1], Michael Kelpel[2,*], Vidal Zakharov[2]

[1] Department of Chemistry, KCG College of Technology, Chennai 600 100, India
[2] Department of Materials Science and Engineering, Technion – Israel Institute of Technology, Haifa 32000, Israel
*Corresponding author: M.kelpel@tx.technion.ac.il

Abstract. Using lignin residue after enzymatic hydrolysis as raw material, resultant lignin-based porous carbon materials were constructed by optimizing the KOH activation process. A single-step activation approach was utilized to investigate how various parameters—including the carbon-to-alkali ratio, activation temperature, and activation duration—influence the physiochemical performance of lignin-derived porous carbon materials. The specific characteristics of the as-synthesized products were tested. Symmetric supercapacitor devices were constructed with KOH serving as the electrolyte medium to assess the material's cycling durability under prolonged galvanostatic charge-discharge conditions. It can be concluded from the experimental findings that the porous carbon specimen designated as ELC700-2-4, which exhibits a large SSA of 3067 m^2/g and a microscale pore percentage of 62.18%, can be successfully synthesized under the conditions of an activation temperature of 700 °C, a carbon-to-alkali mass rate of 4-to-1, and an carbonization duration of 2 hours. Performance evaluation using a three-electrode configuration reveals that the material exhibits remarkable electro and chemical performance within KOH, delivering a specific capacitance at a current density of 1 A/g with value of 443 F/g. Meanwhile, the ELC700-2-4 electrode achieves a specific capacitance of 250 F/g at 1 A/g and maintains 95.55% of its original capacitance after 10,000 consecutive cycles, reflecting superior cycling stability under repeated charging and discharging processes. At a power density of 500.16 W/kg, the symmetric capacitor shows a high energy density of 8.6 W·h/kg.

Keywords: *Lignin; KOH activation; Porous carbon; Supercapacitorn*

Received on 20 Feb 2023, Accepted on 05 Apr 2023, Published on 25 April 2023

1 Introduction

The overexploitation and combustion of fossil fuels have given rise to severe ecological degradation and the depletion of energy reserves [1]. Therefore, developing environmentally friendly, low-carbon emission renewable energy, and effectively improving resource utilization efficiency have attracted widespread attention [2]. Compared to traditional batteries, supercapacitors can be charged and discharged rapidly, and possess excellent chemical stability and safety. The main components of a supercapacitor include electrode materials, separator, current collector, and electrolyte, where the supercapacitor primarily comprises four key constituents: the electrode substance, electrolytic solution, conductive substrate, and insulating membrane. Among these, the electrochemical characteristics and structural change of the material serve as the decisive factor governing the overall efficiency and capacitive behavior of the electric double-layer capacitor (EDLC). The electrochemical characteristics exhibited by the electrode substance fundamentally govern the operational efficacy of electric double-layer capacitors (EDLCs). Owing to their exceptional attributes—including substantial specific surface regions, well-developed porous architectures, and superior electrical conductivity—carbon-based substances have emerged as highly prospective candidates for EDLC electrode applications [3-4]. Typical carbon-based electrode materials employed in EDLCs consist of porous carbon, carbon nanotubes, and graphene. Currently, carbon materials in EDLCs mainly originate from resins, asphalt, and tar, which are directly or indirectly dependent on fossil resources. Therefore, developing new electrode materials based on natural biomass carbon sources has become key to achieving a green transition in energy storage technology.

Lignin represents one of the most plentiful natural macromolecules on Earth, ranking only behind cellulose in terms of natural reserves [5]. Lignin has a high mass fraction of carbon (55%-65%) and possesses performance such as good thermal stability, biodegradability, oxidation resistance, and hardness. Furthermore, the structure of lignin contains a large number of aromatic rings, phenolic hydroxyl groups, carbon-carbon coupling, double bonds, and other active functional groups. Such structural and chemical versatility provides lignin with notable advantages when used as electrode material for supercapacitors and functionally specialized batteries. The KOH activation technique acts as a key pore-forming approach, playing a vital role in regulating the porous structure of lignocellulose-derived carbon materials. To illustrate, Dong and colleagues [6]The researchers employed floral biomass derived from hibiscus plants as the precursor substance, utilizing potassium hydroxide as the chemical activating agent to synthesize lignin-derived porous carbonaceous materials through a sequential process involving thermal carbonization followed by chemical activation treatment. Increasing the KOH-to-precursor ratio contributed to the expansion of pores inside the carbon structure, while significantly boosting the gravimetric capacitance of the biogenic carbon up to 216 F/g. while retaining outstanding cycling stability, with 90.4% of the original capacitance being maintained. Zhang and co-workers [7] utilized agricultural residue from maize cobs as the feedstock, employing potassium hydroxide as the activating reagent to fabricate lignin-rich porous carbon through a sequential dual-stage process comprising initial pyrolysis followed by alkaline activation. Augmentation of the alkali activator dosage led to a pronounced proliferation of microporous structures with diameters below 2 nm. Relative to the pristine untreated precursor, the activated carbon exhibited a remarkable 253% enhancement in gravimetric capacitance, attaining a value of 188 F/g while demonstrating robust electrochemical stability with 90.1% capacitance retention.

The microporous architecture of carbonaceous materials exhibits a strong correlation with their electrochemical characteristics, whereas mesoporous and macroporous networks function as the primary conduits facilitating ionic diffusion and mass transport [8]. Nevertheless, mesoporous and macroporous configurations demonstrate comparatively limited capabilities for charge accumulation. Microporous domains, constituting a critical constituent of the overall porous framework, possess the dual functionality of accommodating substantial charge storage while simultaneously offering adequate spatial volume to facilitate rapid ionic migration and transport kinetics. Consequently, carbonaceous materials featuring a rationally engineered microporous architecture with optimal pore distribution are anticipated to deliver both elevated SSA and enhanced gravimetric capacitance [9-10]. In recent years, substantial scholarly attention has been devoted to elucidating the intricate correlations between porous architectures and the resultant physicochemical performance of materials. To illustrate, Zhang and co-authors [11] successfully reconciled the trade-off between power delivery capability and energy storage capacity through the fabrication of porous carbonaceous materials featuring precisely controllable pore configurations. In another investigation, Xie and colleagues [12] elucidated the intricate structure-function correlations governing the interplay between porous architectures and the electrochemical behavior of carbon-based electrodes in supercapacitor applications, employing a synergistic approach combining operando characterization techniques with computational modeling. Nevertheless, achieving fundamental manipulation of the porous architecture in carbonaceous materials through meticulous regulation of synthetic parameters, coupled with comprehensive elucidation of how such structural modulation influences electrochemical performance, continues to represent a critical domain necessitating thorough systematic investigation and sustained scholarly inquiry in contemporary research endeavors. Based on this, this paper uses enzymatic hydrolysis lignin as raw material and adopts an efficient KOH activation technique to prepare lignin-based porous carbon materials. Through systematic manipulation of pivotal synthetic variables, including the mass proportion between enzymatically hydrolyzed lignin and potassium hydroxide (commonly referred to as the ratio of C-to-base), the carbonization temperature, and the resistance time of thermal treatment, precise governance over the relative proportion of microporous to mesoporous domains within the resultant carbonaceous framework can be successfully realized, enabling systematic investigation into how these processing variables influence the surface structure and pore architectural characteristics of the derived products.

Building upon these findings, the as-synthesized lignin-derived porous carbon specimens were subjected to comprehensive electrochemical characterization, thereby facilitating deeper insight into the intrinsic correlations between structural porosity and electrochemical behavior, thereby furnishing robust theoretical foundations to guide the rational design and performance optimization of porous carbonaceous electrode materials.

2 Materials and Methods

2.1 Reagents used

Enzymatic hydrolysis lignin (EL) was provided by SDIC Advanced Biofuels Co., Ltd.; potassium hydroxide (KOH), absolute ethanol (C_2H_6O, ϕ=99.7%), polytetrafluoroethylene, acetylene black, nickel foam (thickness 1.7 mm) and nitrogen gas (N_2) were purchased from Sigma Aldrich.

2.2 Preparation of Lignin Porous Carbon

Enzymatic hydrolyzed residual lignin precursor was thoroughly blended with potassium hydroxide and subsequently transferred into an alumina ceramic crucible. Under a continuous N_2, the thermal treatment process was started from 15 °C up to a final temperature of 700 °C. At a controlled rate of 5 °C per minute, followed by a two-hour isothermal hold, and cooled back to 15 °C under the same inert gas environment. The resulting lignin-derived carbonaceous product was initially subjected to acid leaching using a 2 M hydrochloric acid solution, subsequently purified through exhaustive washing with deionized water until the effluent attained neutrality,and ultimately subjected to desiccation in a forced-air drying chamber maintained at 105 °C to yield the finalized specimen. The obtained lignin-derived carbon sample was first subjected to acid washing treatment with 2 mol/L HCl solution, then rinsed repeatedly with deionized water until the filtrate became neutral, prior to being dried at 105 °C to yield final product. The influence of different carbonization temperatures (T=650, 750, 800 °C) on the performance of the catalyst (activator) during the carbonization process of ELC700-2-4 was investigated. Samples prepared under different carbonization temperature conditions were named ELC650-2-4, ELC750-2-4, and ELC800-2-4, respectively. Furthermore, the influence of different activation times (t=1, 1.5 h) during the carbonization process of ELC700-2-4 on the performance of the catalyst (activator) was investigated. Samples prepared under different activation times were named ELC700-1-4 and ELC700-1.5-4, respectively.

2.3 Analysis of Sample properties

The surface topography and microstructural features of the as-prepared porous carbon specimens (designated as ELCs) were examined via scanning electron microscopy (SEM, Carl Zeiss AG, Germany). Crystalline arrangement, degree of graphitic ordering within the ELC samples were analyzed employing an X-ray diffractometer (Smart Lab, 9 kW, Rigaku Corporation, Japan) in conjunction with a Raman spectroscopic system (DXR Series, Thermo Fisher Scientific, USA). The morphological characteristics, including SSA and pore size analysis of the prepared porous carbon products, were quantified through nitrogen adsorption-desorption measurements performed using an automated porosity analyzer (Micromeritics, USA).The SSA of the porous carbon specimens was determined through application of the BET theoretical model, utilizing an automated physisorption analyzer. The micropore size distribution was evaluated through application of the Horvath-Kawazoe (HK) theoretical approach.

2.4 Electrochemical Performance Testing of Samples

The ELC constituents were blended with acetylene carbon black (employed as the conductive phase) and polytetrafluoroethylene (utilized as the polymeric binder) according to an 8:1:1 weight ratio. A controlled volume of ethanol was subsequently incorporated to enable comminution and homogenization, continuing until a thick, flowable suspension was achieved. This homogeneous mixture was uniformly spread onto nickel foam current collectors (measuring 1 cm by 2 cm) and subsequently subjected to prolonged desiccation under reduced pressure at 60 °C for a duration of twelve hours. The nickel foam substrates bearing the deposited active layer were positioned within a die-press apparatus and compacted into consolidated electrode laminates under an applied mechanical stress of 10 megapascals. The electro and chemical performance of the as-prepared porous carbon peoducts were assessed using half-cell and full-cell configurations, utilizing a 6 mol/L aqueous KOH as the electrolyte solution. For the three-electrode configuration, the as-fabricated carbon electrode functioned as the working electrode, while the mercury/mercuric oxide couple provided the reference potential and a platinum foil served as the auxiliary electrode. Within the dual-electrode configuration, two electrode laminates possessing identical mass loadings were employed as the respective positive and negative terminals within a coin-cell architecture, thereby constructing a symmetric electro and chemical double-layer capacitor, with a cellulose-based membrane interposed between the electrodes to facilitate ionic conduction while maintaining

electronic isolation.

Cyclic voltammetry (CV) analysis were carried out to assess the charge storage behavior of porous carbon electrodes. Galvanostatic charge-discharge (GCD) analysis was utilized to evaluate rate property and long-term cycling capacity of the electrode materials. Electrochemical impedance spectroscopy (EIS) was employed to evaluate the resistive and capacitive properties of the system. All electrochemical assessments, encompassing CV, GCD, and EIS analyses, were executed employing a CHI760E potentiostat/galvanostat (Chenhua Instruments, China).The potential window for cyclic voltammetry measurements spanned from -1 to 0 V, with potential sweep rates varied between five and one hundred mV/s. Alternating current analysis was conducted at the equilibrium open-circuit potential, covering a spectrum ranging from 10^5 to 10^{-2} Hz. Galvanostatic charge-discharge evaluation was performed within the potential interval of -1 to 0 V, employing current densities spanning from 0.1 to 5 A/g. The gravimetric specific capacitance C (F/g) for an individual electrode was determined using the following equation: $C = (I\Delta t) / (m\Delta V)$

where I (A) denotes the applied current, Δt (s) corresponds to the discharge duration, and m (g) refers to the mass of active material loaded on the electrode, while ΔV (V) indicates the potential window excluding the ohmic voltage drop (IR drop) during the discharge period.I notice there is a discrepancy in your text - you mentioned "LACT-R electrodes" which appears to be a specific material designation not referenced in previous context (the earlier text discussed "ELCs"). I will proceed with the paraphrasing assuming this is the correct terminology:

For the symmetric cell configuration, two LACT-R electrodes exhibiting equivalent active material loadings (approximately 2.5 mg per electrode) were selected as the respective anode and cathode and assembled into a coin-type electrochemical capacitor within a CR2032 cell housing, with the two electrodes physically isolated by a porous separator membrane. The total specific capacitance (Ct), single-electrode specific capacitance (Cs), and energy density (E) along with power density (P) of the porous carbon material were computed using the following formulas:

$C_s = 4\ C_t$

$E = (C_t\ \Delta V^2) / (3.6 \times 2)$

$P = 3600E / \Delta t$

where (M) (g) denotes the total mass of the active substance within the supercapacitor, and ΔV stands for voltage variation obtained from the GCD measurement after deducting the voltage drop during the discharge process.

3 Results and Discussion

3.1 Morphological and Structural properties of ELCs

The microstructural features of the ELC specimens are presented in Figure 1. As depicted in panels (A) through (E) of Fig. 1, the KOH-activated samples exhibit a pronounced porous texture characterized by abundant voids and cavities distributed throughout the carbon matrix, attributable to the chemical etching and gasification reactions induced by the alkaline activator. As the carbon-to-alkali ratio increases from 1:1 to 4:1, more pores are formed in the ELCs skeleton, making the shape of the ELCs more irregular. Among them, ELC700-2-4 has a more developed pore structure, thinner pore walls, and more interconnected pore walls, resembling a honeycomb shape (Fig. 1(D)). This special porous structure can provide efficient ion transport and electron transfer. When the carbon-to-alkali ratio is 5:1, the pore structure of ELC700-2-5 partially collapses (Fig. 1(E)), which is due to excessive KOH etching.

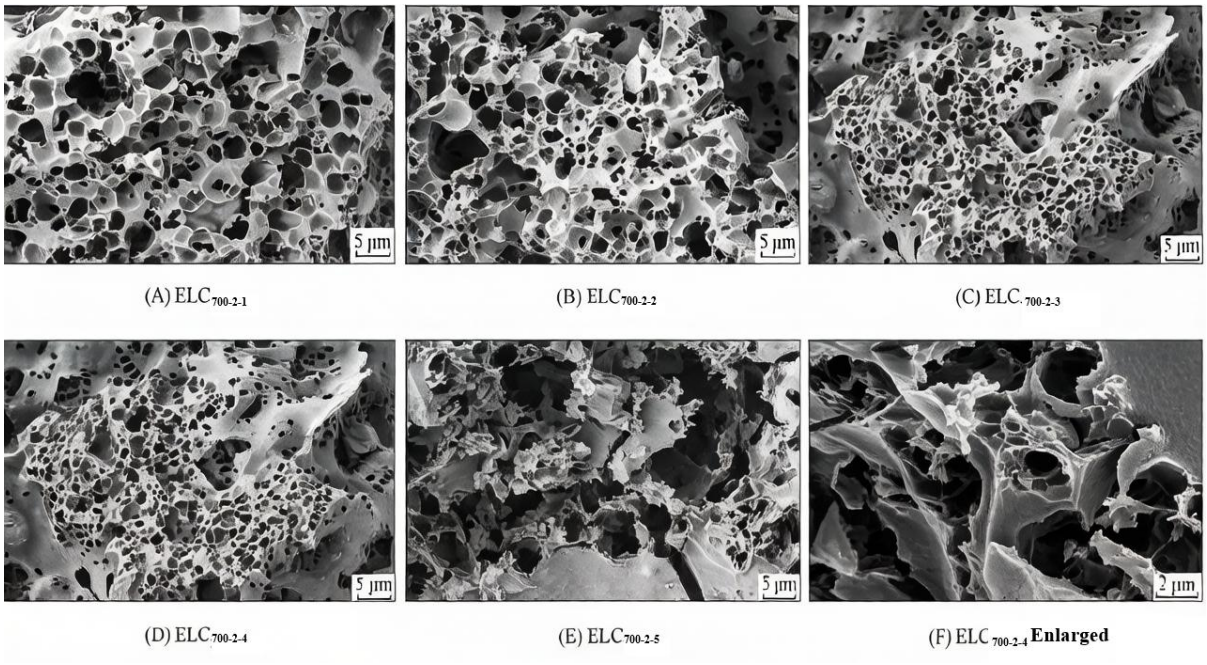

Figure 1 SEM of carbon materials

As seen in Fig. 1(F), ELC700-2-4 exhibits a typical three-dimensional interconnected porous structure, resulting from the pore-forming effect of gaseous products like CO_2 and water vapor generated during the activation process [13]. This is consistent with the classic KOH activation mechanism: under high-temperature conditions, KOH selectively removes carbon atoms through oxidation etching reactions, thereby increasing the material's porosity [14]. The formation of micropores is mainly attributed to the intercalation and etching effect of K^+, while mesopores mainly arise from structural reorganization caused by gas escape. The elemental mapping diagram of ELC700-2-4 is shown in Fig. 2. As seen in Fig. 2, C, N, and O elements are present in ELC700-2-4.

The crystalline structure and degree of graphitic ordering within the ELC samples were examined through X-ray diffraction and Raman spectroscopic analyses, with the resultant data presented in Figure 3. As illustrated in panel (A) of Fig. 3, the ELC materials display broad, low-intensity diffraction signals centered at approximately 23° and 44°, which can be indexed to the (002) and (100) reflections of turbostratic carbon, respectively,This observation confirms the predominantly amorphous nature of the ELC materials, characterized by a lack of long-range crystallographic order. Such disordered atomic arrangements are advantageous for electrochemical applications, as they facilitate enhanced accessibility and diffusion pathways for electrolyte ions [15]. With increasing carbon-to-alkali ratio, the diffraction peak at 44° progressively diminishes in intensity, suggesting a higher degree of structural disorder within the porous carbon framework,which can be attributed to the generation of substantial structural defects within the carbon matrix during KOH activation, thereby disturbing the ordered arrangement of carbon atoms [16].As depicted in Fig.3(B), all ELC samples show two distinct specific peaks located at approximately 1340 and 1580 cm^{-1}, which are assigned to D band (defect-induced mode) reflecting disorder of structure and G band (graphitic mode) rose from in-plane sp^2 carbon vibrations in hexagonal lattice structures, respectively [17]. The intensity ratio between the D and G (ID/IG) serves as a quantitative metric for assessing the degree of structural disorder and the extent of graphitic ordering within carbonaceous materials. An elevated ID/IG value signifies a greater concentration of structural imperfections and a diminished degree of graphitic crystallinity within the carbon specimen [18].As the carbon-to-alkali ratio increases, ID/IG gradually decreases, and graphitization increases; but when the carbon-to-alkali ratio is too high, the graphitization degree reduces. Therefore, an appropriate carbon-to-alkali ratio is beneficial for promoting the graphitization degree of ELCs, while an excessive carbon-to-alkali ratio can cause pore structure collapse.

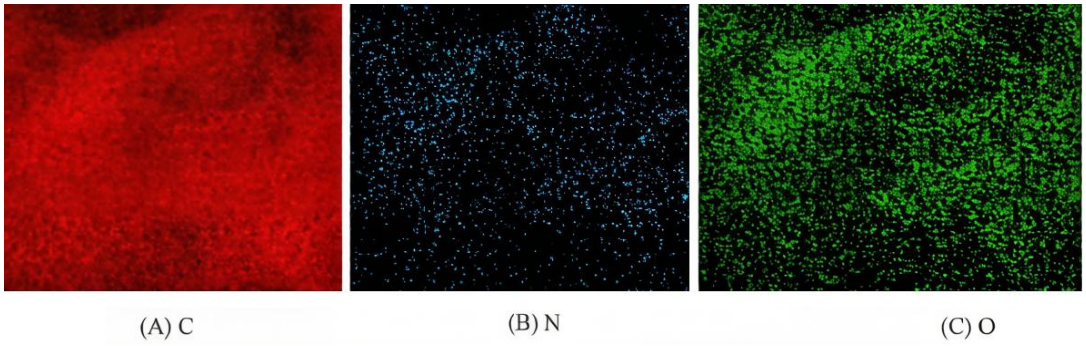

Figure 2 Mapping diagram of ELC700-2-4 elements in SEM-EDS

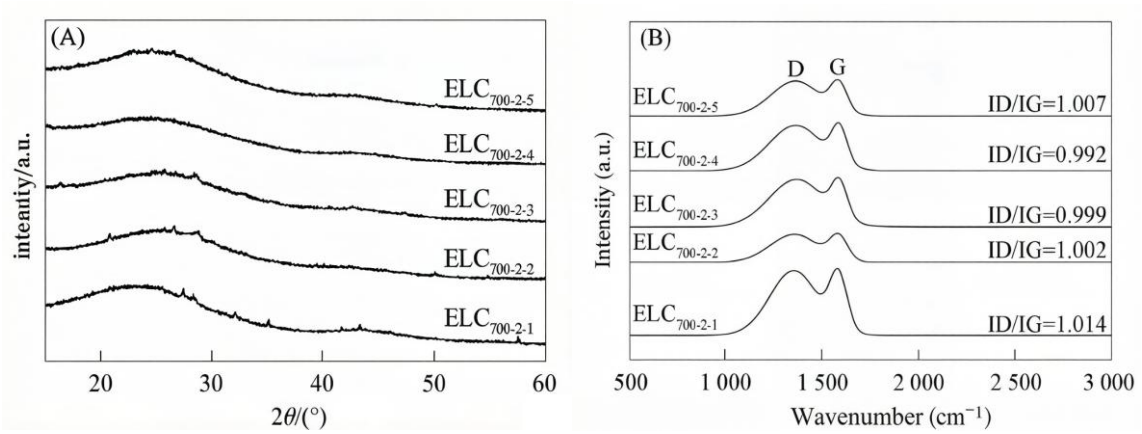

Figure 3 XRD analysis (A) and Raman analysis (B) of porous samples

3.2 Electro-and-chemical Performance

3.2.1 Ratio of Enzymatic Hydrolysis Lignin to KOH

Table 1 Pore parameters of carbon materials

Sample	S_{BET} / ($m^2 \cdot g^{-1}$)	V_{total} / ($cm^3 \cdot g^{-1}$)	$V_{micropore}$ / ($cm^3 \cdot g^{-1}$)	($V_{micropore}$ / V_{total}) / %	Diameter / nm
ELC700-2-1	570	0.25	0.21	85.61	1.75
ELC700-2-2	2,219	0.97	0.89	90.59	1.76
ELC700-2-3	3,128	1.78	1.19	66.78	2.27
ELC700-2-4	3,067	1.82	1.14	62.18	2.38
ELC700-2-5	2,912	1.91	1.03	53.97	2.62
ELC650-2-4	2,885	1.66	1.20	78.14	2.30
ELC750-2-4	3,344	2.22	1.13	50.94	2.65
ELC800-2-4	3,283	2.52	0.66	26.16	3.07
ELC700-1-4	3,200	1.98	1.26	63.68	2.48
ELC700-1.5-4	3,080	1.91	1.10	57.39	2.48

Dosage of activating agent exerts a predominant influence on the development and architectural features of the porous network within carbonaceous materials. Figures 4(A) and 4(B) display the N_2 adsorption–desorption isotherms and the resulting pore structural curves of the carbon products prepared at different carbon-to-alkali ratios, respectively. As depicted in Fig. 4(A), the N_2 adsorp-desorp isotherms for all ELC samples showed typical Type I profiles, indicative of predominantly microporous materials. Within the low pressure domain ($p/p_o < 0.02$), adsorbed volume for the various porous carbon specimens undergoes a steep ascent and rapidly approaches equilibrium saturation, signifying the prevalence of abundant microporous structures within these materials. As illustrated in Fig. 4(B), the micropore population in the ELC samples is predominantly focused on the narrow distribution of 0.35 to 0.70 nm. These ultrafine pores make a substantial contribution to the overall capacitive response of porous carbon electrodes, particularly when employing aqueous potassium hydroxide as the electrolytic medium. Additionally, specimens ELC700-2-3, ELC700-2-4, and ELC700-2-5 exhibit pronounced H4-type loops within intermediate pressure of their sorption isotherms, which is characteristic of the presence of mesoporous structures with diameters ranging from 2 to 5 nm. Mesoporous structures serve dual functions by facilitating expedited ionic transport through well-defined diffusion pathways and concurrently diminishing the effective diffusion distance, thereby alleviating pore congestion resulting from excessive ion accumulation within microporous domains. Different pore of ELC products cause significant differences in their SSA values. The content of activator KOH plays a significant role in the porous structure of carbon materials, with results listed in **Table 1**.

As shown in **Table 1**, when the carbon-to-alkali ratio rises from 1:1 to 4:1, the SSA (S_BET) of the ELC samples exhibits a gradual increase. The SSAs of ELC700-2-1, ELC700-2-2, and ELC700-2-3 are measured to be 570, 2219, and 3128 m²/g, respectively. When the KOH amount continues to increase, the SSAs of samples ELC700-2-4 and ELC700-2-5 slightly decrease to 3,067 and 2,912 m²/g, respectively. The cumulative pore volume (V_total) exhibits a progressive augmentation across the five porous carbon specimens as the potassium hydroxide dosage is incrementally elevated.Microporous structures significantly enhance charge storage capability at the electrode-electrolyte interface,thereby substantially improving the energy density of electric double-layer capacitors.Their confined pore size can effectively increase the surface charge density through quantum confinement effects, thereby achieving fast charge-discharge kinetics. However, excessively small pores may lead to ion sieving effects, especially during fast charge-discharge processes, hindering the diffusion path of electrolyte ions (e.g., K^+, OH^-), resulting in specific capacitance decay. Mesoporous structures facilitate ion transport dynamics through the formation of a three-dimensionally interconnected pore network,I notice this appears to be a continuation of a scientific paper about porous carbon materials for supercapacitors. However, an excessive mesopore content will diminish the overall SSA of the material, resulting in reduced specific capacitance under low current densities.Consequently, optimization of the micropore-to-mesopore proportion is advantageous for reconciling the competing requirements of extensive surface area accessibility and rapid ionic mobility, ultimately enabling the simultaneous attainment of elevated gravimetric capacitance and superior rate capability.Figures 4(C) and 4(D) illustrate the cyclic voltammetry curves tested at a scan rate of 50 mV/s and the galvanostatic charge-discharge plots measured at a current density of 1 A/g, respectively. As depicted in Fig. 4(C), at the specified scan rate of 50 mV/s, the voltammetric responses for all samples prepared under varying carbon-to-alkali ratios display approximately rectangular configurations, which is characteristic of ideal capacitive behavior and confirms the predominantly electric double-layer charge storage mechanism of the ELC electrode materials.Among these specimens, ELC700-2-4 exhibits the most extensive voltammetric loop area alongside a configuration most closely approximating an ideal rectangular geometry, which signifies that this particular porous carbon possesses the highest gravimetric specific capacitance and superior charge accumulation capability,an observation that can be attributed to its more favorable hierarchical porous architecture facilitating enhanced electrochemical performance.As illustrated in Fig. 4(D), the galvanostatic charge-discharge profiles for all ELC specimens exhibit an approximately symmetric triangular morphology.The linear and symmetric profile characteristics signify that these materials demonstrate outstanding electrochemical reversibility coupled with rapid charge-discharge kinetics.ELC700-2-4 exhibits the most extended discharge duration, indicative of its superior capacitive characteristics among all tested specimens. These findings align well with the CV analysis outcomes. The gravimetric specific capacitances for ELC700-2-1, ELC700-2-2, ELC700-2-3, ELC700-2-4, and ELC700-2-5 were determined to be 272, 287, 342, 443, and 300 F/g, respectively.Fig. 4(E) presents the Nyquist plots obtained from electrochemical impedance spectroscopy measurements for the ELC electrodes.In the high-frequency domain, the intersection point of the impedance curve with the real axis corresponds to the equivalent series resistance (R_s),the magnitude of which indicates the overall internal resistance inherent to the

electrochemical system.The R_s values for ELC700-2-1, ELC700-2-2, ELC700-2-3, ELC700-2-4, and ELC700-2-5 electrodes are 0.55, 0.3, 0.6, 0.58, and 0.59 Ω, respectively. ELC700-2-2 has the smallest R_s value, which may be related to its higher degree of graphitization. The diameter of the semicircular loop in the high-frequency region is directly related to the value of the charge-transfer resistance (R_ct).A smaller semicircle indicates lower charge-transfer resistance and faster interfacial charge transfer kinetics.The R_ct values for ELC700-2-1, ELC700-2-2, ELC700-2-3, ELC700-2-4, and ELC700-2-5 electrodes are 0.0855, 0.17, 0.12, 0.0851, and 0.13 Ω, respectively. Sample ELC700-2-4 has the smallest R_ct value, which may be due to the better accommodation of electrolyte ions by the mesopore volume in the material; appropriately increasing the mesoporosity helps reduce the R_ct value. In the low-frequency domain, the approximately vertical line observed for all samples is indicative of predominantly capacitive response characteristics,implying facile accessibility of the electrolyte into the porous network of the ELC electrodes.Typically, a rich pore structure is beneficial for ion storage and rapid transport. The variation of the samples' specific capacitance (C_F) with specific pore volume is shown in Fig. 4(F). As seen in Fig. 4(F), ELC700-2-1 and ELC700-2-2 have lower specific pore volumes and SSAs, hence their capacitive performance is poorer. ELC700-2-3, ELC700-2-4, and ELC700-2-5 have larger specific pore volumes, 1.78, 1.83, and 1.91 cm^3/g, respectively. Although ELC700-2-3 has the largest SSA, as seen from Table 1, most of its SSA comes from micropores. While ELC700-2-5 has the largest total pore volume, its micropore volume ratio is relatively low, only 53.97%, so its specific capacitance is also lower than that of ELC700-2-4. Although ELC700-2-4 has a smaller total pore volume than ELC700-2-5, its micropore volume shows an increasing trend. This structural feature gives ELC700-2-4 a higher specific capacitance value. This finding not only confirms the crucial role of the microporous structure in capacitive behavior but also suggests that tuning the micropore–mesopore ratio can effectively enhance the overall performance of the material.

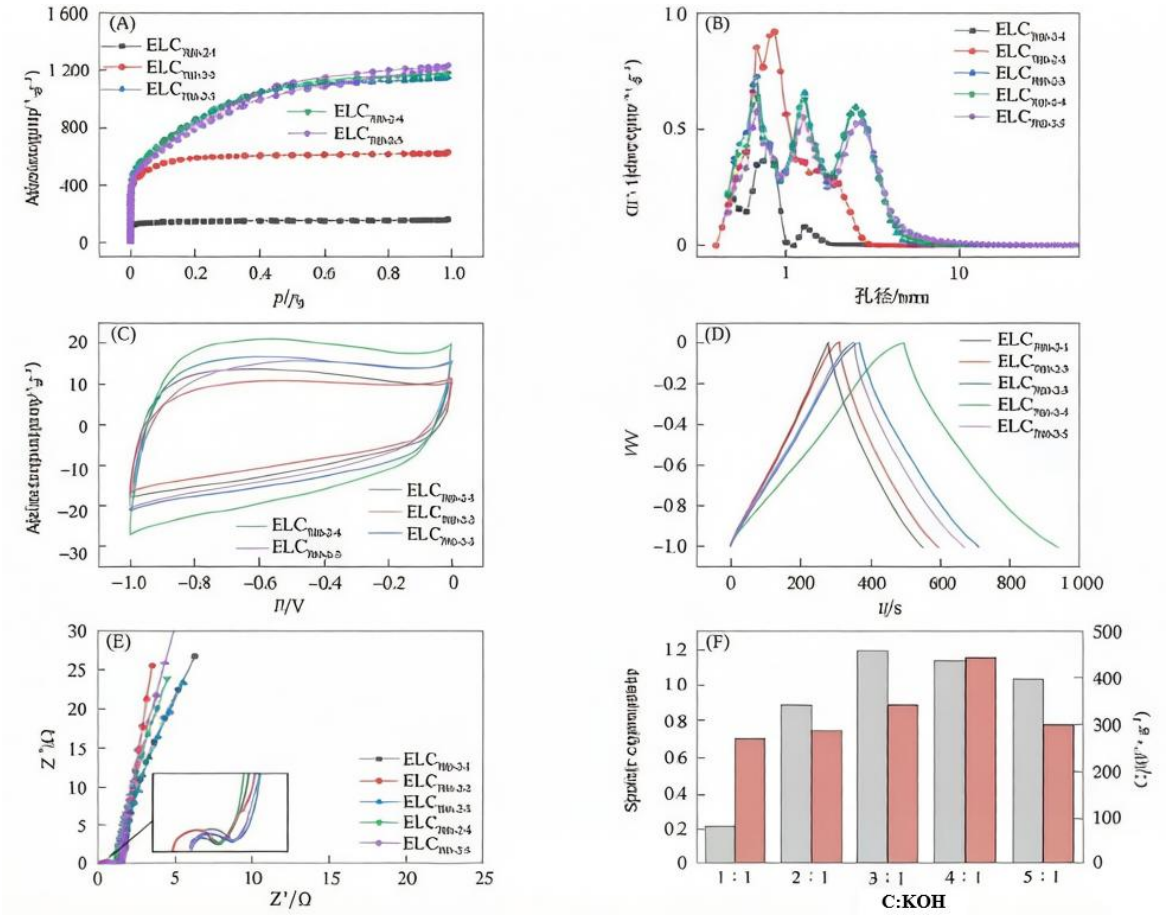

Figure 4 N_2 adsorption-desorption isotherms (A), pore size distribution curves (B), CV curves at 50 mV/s (C), GCD curves at 1 A/g (D), electrochemical impedance spectroscopy (E) and pore size distribution and specific capacitance (F) of samples with different carbon-alkali ratios

3.2.2 Effect of Carbonization Temperature

Thermal carbonization temperature represents another critical parameter governing the evolution of porous architecture and the resultant electrochemical behavior. The N_2 sorption isotherms for carbon specimens prepared at various carbonization temperatures are presented in Fig. 5. As illustrated in Fig. 5(A), the nitrogen sorption isotherms for all ELC specimens exhibit typical Type I characteristics,indicative of a predominant microporous architecture in these carbonaceous materials. As illustrated in Fig. 5(B), the micropore population in the ELC samples is predominantly concentrated within the range of 0.2 to 2 nm, with the majority falling between 0.35 and 0.7 nm. Additionally, specimens ELC750-2-4 and ELC800-2-5 exhibit pronounced H4-type hysteresis loops within the intermediate relative pressure region of their sorption isotherms, signifying the presence of a substantial quantity of mesoporous structures. As temperature raised from 650 °C to 750 °C, the SSA of the ELC samples demonstrates a gradual increase, as summarized in Table 1. The ELC650-2-4, ELC700-2-4, and ELC750-2-4 samples exhibit SSAs of 2,885, 3,067, and 3,344 m²/g, respectively. When the carbonization temperature is further increased above 750 °C, the SSA of the ELC800-2-4 sample slightly decreases to 3283 m²/g.The pore volumes of the four porous carbons all gradually increase with increasing carbonization temperature.

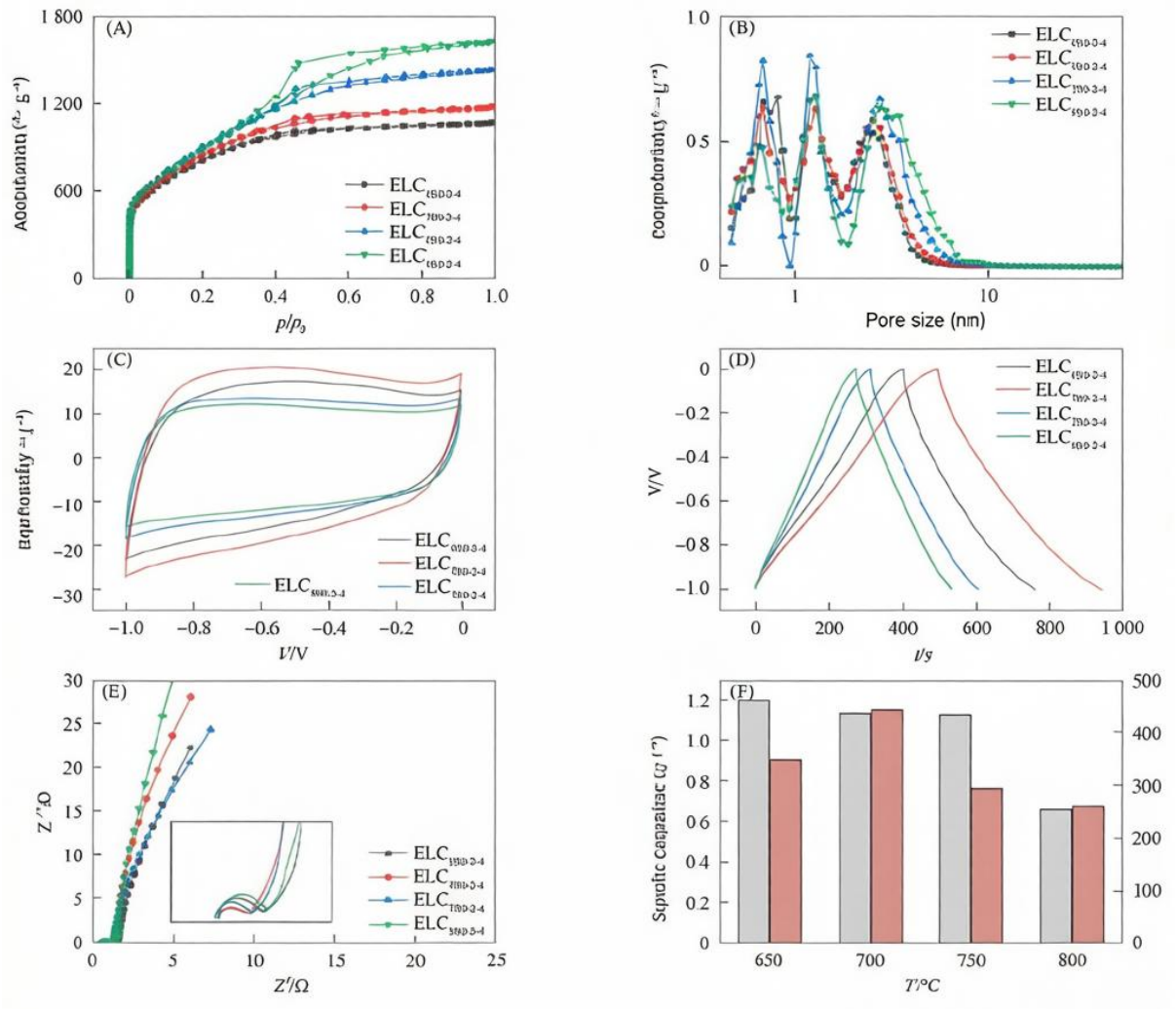

Figure 5 N_2 adsorption-desorption isotherms (A), pore size distribution curves (B), CV curves at 50 mV/s (C), GCD curves at 1 A/g (D), electrochemical impedance spectroscopy (E) and pore size distribution and specific capacitance (F) of samples at different carbonization temperatures

The cyclic voltammograms recorded at a scan rate of 50 mV/s and the galvanostatic charge-discharge profiles obtained at a current density of 1 A/g for the respective samples are presented in Fig. 5(C) and (D),respectively.

As depicted in Fig. 5(C), at a scan rate of 50 mV/s, the CV curves for samples prepared at varying carbonization temperatures all display a near-rectangular morphology,suggesting that the ELC electrode materials exhibit characteristic electric double-layer capacitive behavior. Among these samples,ELC700-2-4 exhibits the largest integrated area under the CV curve and a morphology most closely approximating an ideal rectangular shape. As illustrated in Fig. 5(D), the GCD profiles for all ELC samples display a near-triangular configuration.The linear and symmetric profile characteristics signify that these materials demonstrate outstanding electrochemical reversibility coupled with rapid charge-discharge kinetics [19].This is already a well-paraphrased version.

The remarkable high-rate performance demonstrated by ELC700-2-4 stems from its rationally designed porous architecture, wherein the judicious balance of micro- and mesoporous domains provides plentiful redox-active interfaces while simultaneously facilitating expedited ionic diffusion through shortened transport pathways, thereby maximizing the effective accessibility of the carbonaceous matrix to electrolyte ions [20-21].The discharge duration exhibited by ELC700-2-4 considerably surpasses those of the remaining specimens, corroborating the findings derived from the cyclic voltammetry analysis. Fig.5(E) presents the Nyquist impedance diagrams for the ELC electrodes.The equivalent series resistance (R_s) values determined for the ELC650-2-4, ELC700-2-4, ELC750-2-4, and ELC800-2-4 electrodes are 0.59, 0.58, 0.55, and 0.59 Ω, respectively.The R_ct values for ELC650-2-4, ELC700-2-4, ELC750-2-4, and ELC800-2-4 electrodes are 0.12, 0.085, 0.11, and 0.15 Ω, respectively. Sample ELC700-2-4 has the smallest R_ct value, indicating it has better electrochemical performance and ion transport efficiency.

The variation of the samples' specific capacitance with specific pore volume is shown in Fig. 5(F). From the GCD curves, the specific capacitances of ELC650-2-4, ELC700-2-4, ELC750-2-4, and ELC800-2-4 are 350, 443, 294, and 260 F/g, respectively. The diminished specific pore volume and reduced SSA of ELC650-2-4 contribute to its inferior capacitive performance. ELC700-2-4, ELC750-2-4, and ELC800-2-4 have larger specific pore volumes, 1.83, 2.22, and 2.52 cm^3/g, respectively. Although ELC750-2-4 has the largest SSA, as seen from Table 1, most of its SSA comes from micropores. While ELC800-2-4 has the largest total pore volume, its micropore volume ratio is relatively low, only 26.16%, so its specific capacitance is also lower than that of ELC700-2-4. Although the total pore volume of ELC700-2-4 is smaller than that of ELC750-2-4 and ELC800-2-4, its micropore volume is larger. This structural feature gives ELC700-2-4 a higher specific capacitance value. This result not only proves the key role of the microporous structure in capacitive performance but also indicates that optimizing the ratio of micropores to mesopores can improve material performance.

3.2.3 Effect of Carbonization Time

The duration of thermal carbonization represents another critical parameter influencing the evolution of porous architecture and the resultant electrochemical characteristics.The nitrogen sorption isotherms and corresponding pore size distribution profiles for carbon specimens prepared at varying carbonization durations are presented in Fig.6(A) and 6(B), respectively. As depicted in Fig. 6(A), the ELC samples subjected to different carbonization durations all exhibit abundant microporous structures, while the presence of hysteresis loops in their respective isotherms confirms the existence of mesoporous domains across all three materials.As seen in Fig. 6(B), the three materials have a certain amount of mesopores in the 2~5 nm range. Upon extending the carbonization duration from 1 hour to 2 hours, the SSA of the ELC specimens undergoes a progressive diminution, as detailed in Table 1.The ELC700-1-4, ELC700-1.5-4, and ELC700-2-4 specimens possess SSAs of 3,200, 3,080, and 3,067 m^2/g, respectively, while the cumulative pore volume exhibits a progressive reduction with increasing activation time.The cyclic voltammograms recorded at a sweep rate of 50 mV/s and the galvanostatic charge-discharge profiles obtained at a current density of 1 A/g are presented in Figures 6(C) and 6(D), respectively.As depicted in Fig. 6(C), at the specified scan rate of 50 mV/s, the voltammetric responses for all samples subjected to varying activation durations display approximately rectangular configurations, which is characteristic of ideal capacitive behavior and confirms the predominantly electric double-layer charge storage mechanism of the ELC electrode materials.As depicted in Fig. 6(D), across the potential range of 0 to 1 V,the galvanostatic charge-discharge profiles for all samples exhibit nearly symmetrical triangular shapes, indicating excellent electrochemical reversibility.The gravimetric specific capacitances determined for ELC700-1-4, ELC700-1.5-4, and ELC700-2-4 are 337.7, 443, and 374 F/g, respectively. The electrochemical impedance spectroscopy findings are presented in Fig. 6(E).As depicted in Fig. 6(E), the equivalent series resistance (R_s) values for the ELC700-1-4, ELC700-1.5-4, and ELC700-2-4 electrodes are determined to be 0.55, 0.58, and 0.60 Ω, respectively, while the

corresponding charge transfer resistance (R_ct) values are 0.13, 0.12, and 0.085 Ω, respectively.Specimen ELC700-2-4 exhibits the minimal charge transfer resistance, which can be attributed to the enhanced accessibility and accommodation of electrolyte ions facilitated by the mesoporous volume within its structural framework,thereby facilitating expedited interfacial charge transfer kinetics. In the low-frequency region, the nearly vertical slope of the impedance curve reflects the ideal capacitive behavior of the electrode materials, suggesting unobstructed diffusion of electrolyte ions into the porous structure. The correlation between the gravimetric specific capacitance and specific pore volume for the various specimens is illustrated in Fig. 6(F). The specific pore volumes of ELC700-1-4, ELC700-1.5-4, and ELC700-2-4 are 1.98, 1.91, and 1.83 cm^3/g, respectively. As evident from Table 1, the majority of the SSA for ELC700-2-4 is contributed by micropores. This result again demonstrates the important role of the microporous structure in enhancing capacitive performance, indicating that regulating the ratio of micropores to mesopores can improve the overall capacitive performance of the material.

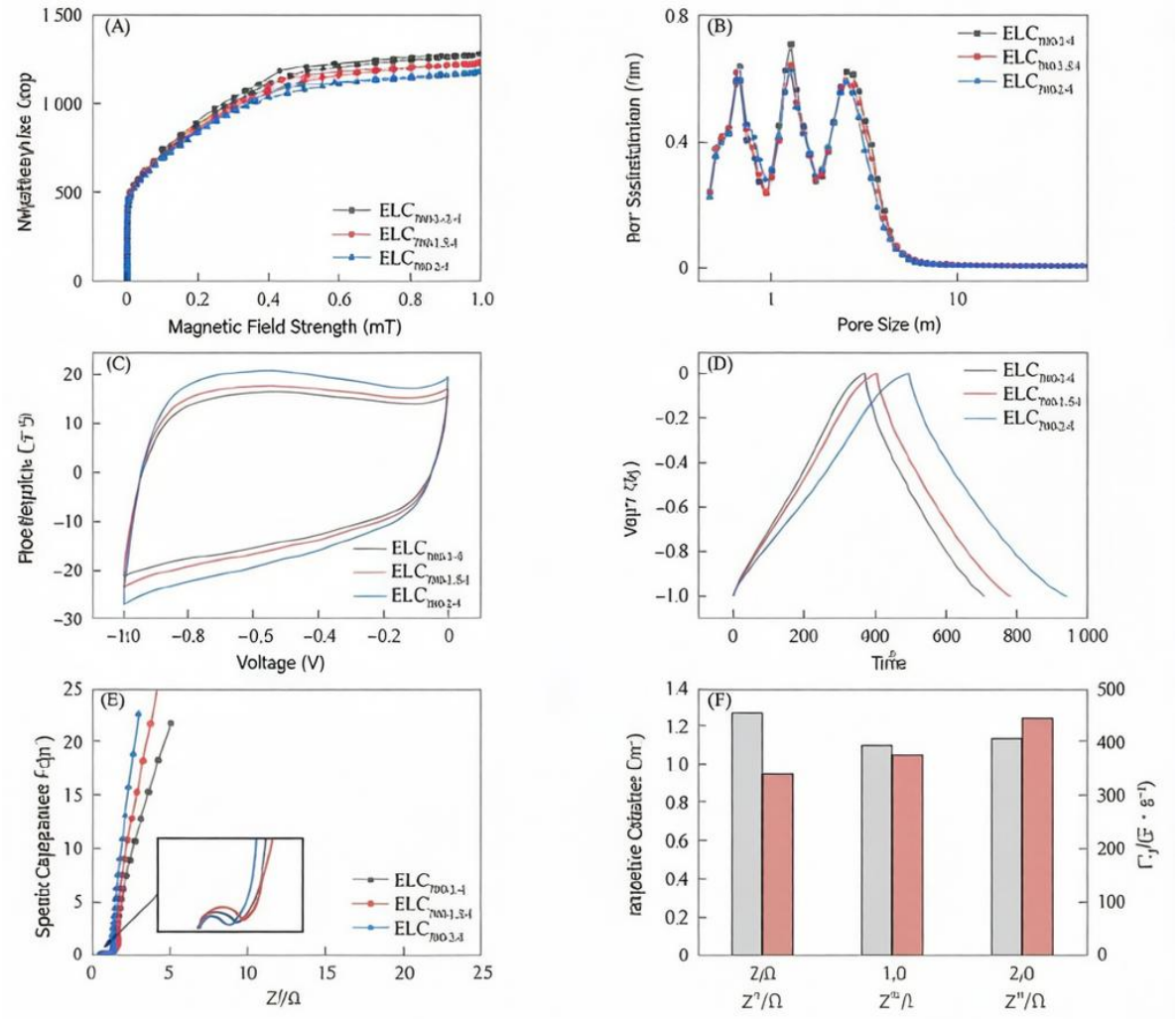

Figure 6 N_2 adsorption-desorption isotherms (A), pore size distribution curves (B), CV curves at 50 mV/s (C), GCD curves at 1 A/g (D), electrochemical impedance spectroscopy (E) and pore size distribution and specific capacitance (F) of samples at different carbonization time

3.3 Symmetrical Supercapacitor Based on ELC700-2-4

To comprehensively assess the practical viability of ELC700-2-4, symmetric electrochemical capacitors were fabricated employing ELC700-2-4 electrodes with aqueous KOH serving as the electrolytic medium, and subsequently evaluated within a two-electrode configuration.The electrochemical characterization findings are presented in Figure 7, with panel (A) displaying the cyclic voltammograms for the ELC700-2-4 electrode recorded

at scan rates ranging from 5 to 100 mV/s.As depicted in Fig. 7(A), the ELC700-2-4 electrode maintains approximately rectangular voltammetric profiles across the entire range of sweep rates, which is indicative of near-ideal electric double-layer capacitive behavior.The rectangular morphology of the voltammetric responses reflects the efficiency of electrolyte ion diffusion within the porous electrode architecture.A more ideal rectangular configuration signifies enhanced ionic diffusion kinetics within the electrode material.This is already well-paraphrased. Here is a slightly alternative version:

As shown in Fig. 7(B), across current densities from 0.5 to 10 A/g, the charge-discharge profiles demonstrate pronounced linear symmetry with negligible voltage drop, indicating the ELC700-2-4 electrode maintains superior reversibility during cycling. Due to the relatively high equivalent series resistance typical of coin-cell assemblies, the measured specific capacitance values are somewhat moderate, as referenced in [22–23].Accordingly, the gravimetric specific capacitance reaches 273 F/g at 0.5 A/g, and remains 221.8 F/g at a high current density of 10 A/g, corresponding to a capacitance retention rate of 81.25%.Energy density serves as a critical metric for assessing the energy storage capability of supercapacitor devices.The Ragone plot depicting the energy-power characteristics of the ELC700-2-4 supercapacitor is presented in Fig.7(C). As illustrated in Fig. 7(C), at a power density of 4998.12 W/kg, the corresponding energy density attains 7.4 W·h/kg. The energy density achieved by the ELC700-2-4 supercapacitor surpasses those reported for other symmetric supercapacitors employing carbon-based electrodes. The exceptional electrochemical performance demonstrated by this material highlights its promising viability as an electrode candidate for supercapacitor applications [7, 24-29].At a current density of 1 A/g, the ELC700-2-4 electrode maintains a high specific capacitance value following 10,000 galvanostatic charge-discharge cycles,retaining 95.55% of its initial specific capacitance, which demonstrates the excellent cycling stability of the ELC700-2-4 electrode in 6 M KOH electrolyte [30].

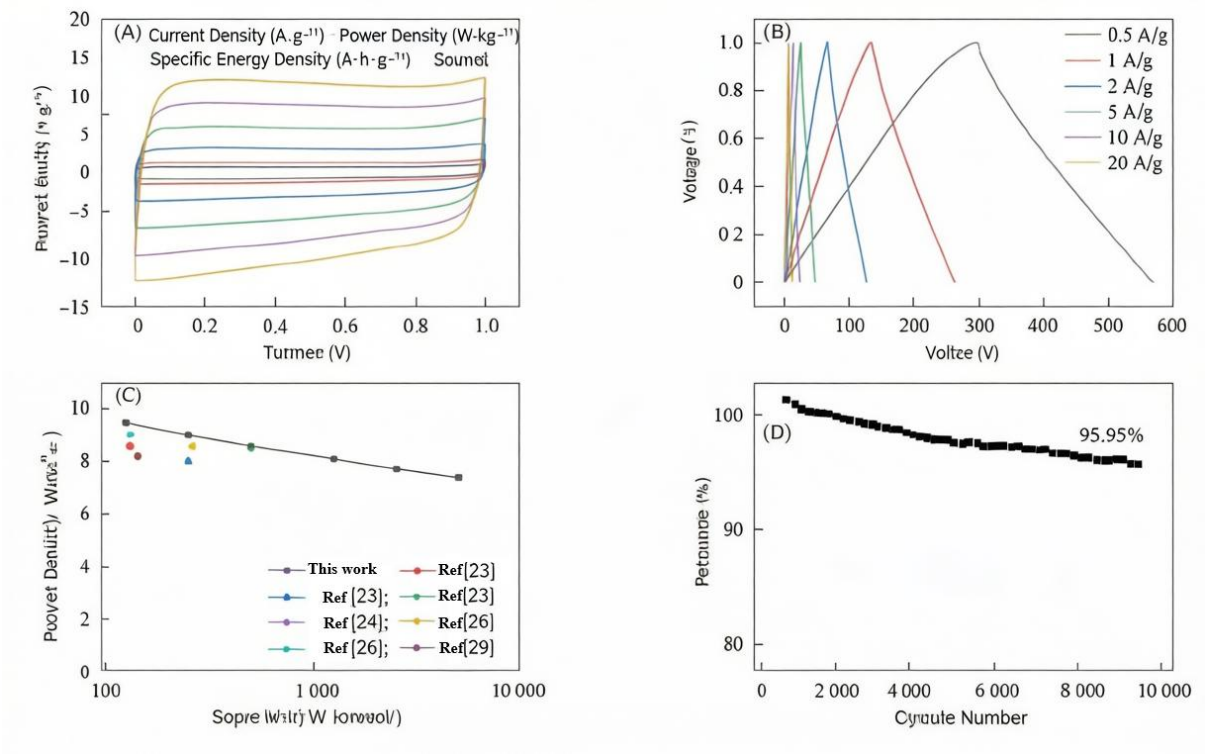

Figure 7 CV curves at different scan rates (A), GCD curves at different current densities (B), Ragone plot (C) and capacitance retention rate (D) of ELC

In conclusion, the present investigation utilizes enzymatically hydrolyzed lignin as the precursor material and adopts a facile one-step KOH carbonization strategy to synthesize lignin-derived porous carbonaceous materials.Through systematic manipulation of the KOH carbonization parameters, precise control over the porous architecture of the resulting carbon materials is successfully realized.This is already well-paraphrased.

Here is a slightly alternative version:

The experimental results reveal that at a pyrolysis temperature of 700 °C, variations in the carbon-to-alkali proportion have limited impact on the graphitic crystallinity of the ELCs; as the alkali loading increases, the SSA initially rises before declining, the microporous content gradually diminishes, and the mean pore dimension progressively expands; when maintaining a 4:1 carbon-to-alkali ratio, increasing the thermal treatment temperature promotes greater graphitization while the SSA exhibits a volcano-type dependence on temperature; among all prepared samples, ELC700-2-4 demonstrates a SSA of 3,067 m²/g.This is already well-paraphrased. Here is a slightly alternative version:

Electrochemical evaluation demonstrates that the specific capacitance exhibits a non-monotonic dependence on both carbon-to-alkali proportion and pyrolysis temperature, displaying an initial upward trend followed by a downward trajectory as these parameters intensify; in contrast, extending the carbonization period results in continuous capacitance enhancement; the optimized porous carbon ELC700-2-4, synthesized at a carbon-to-alkali ratio of 4:1, a heat treatment temperature of 700 °C, and a holding time of 2 hours, exhibits a specific capacitance of 443 F/g at 1 A/g.The symmetric electrochemical capacitor fabricated utilizing this carbonaceous material demonstrates outstanding energy storage performance; specifically, at a power density of 4,998.12 W/kg, the device achieves an energy density of 7.4 Wh/kg, while maintaining exceptional cycling stability with 95.5% capacitance retention following 10,000 galvanostatic charge-discharge cycles.This research effectively advances the transformation and exploitation of lignocellulosic waste resources, furnishes a practical methodology for fabricating economically viable, high-capability supercapacitor electrode substances, and possesses significant academic importance and engineering potential for promoting the evolution of sustainable energy storage systems.

3.4 Mechanisms for enhanced performance of supercapacitor

This discussion delves into the mechanisms underlying the formation, structure-property relationships, and electrochemical performance of the enzymatic hydrolysis lignin-based porous carbons (ELCs) prepared via KOH carbonization as detailed in the provided document. The fundamental mechanism relies on the synergistic effect between KOH-mediated chemical carbonization, the formation of a hierarchical porous structure, and the electric double-layer capacitance (EDLC) behavior exhibited in aqueous electrolyte. The KOH carbonization mechanism is essentially a gasification and etching reaction that occurs under inert atmosphere at high temperatures ranging from 650 to 800 °C. At these temperatures, KOH decomposes and reacts with the carbon framework of the lignin precursor through a series of redox reactions. Key reactions involve the reduction of KOH to metallic potassium (K) and the oxidation of carbon to produce carbonates (K_2CO_3), along with the generation of gaseous products like H_2, H_2O, and CO_2. The intercalation of metallic K into the carbon lattice creates immense internal pressure, physically expanding and exfoliating the structure, which is a primary driver for microporosity creation. Simultaneously, the gaseous products, particularly CO_2 and H_2O, further etch the carbon walls, enlarging existing pores and creating new ones. This combined chemical and physical effect selectively removes carbon atoms, promoting the formation of porous structures. The precise control over this etching process via parameters like carbon-to-alkali ratio (C/KOH), carbonization temperature, and carbonization time is crucial for tailoring the final pore architecture.

The optimization of these parameters directly dictates the pore structure, which in turn governs electrochemical performance. As the C/KOH ratio increases from 1:1 to 4:1, the availability of KOH for etching rises, leading to a significant increase in SSA (S_BET from 570 to 3128 m²/g) and total pore volume. However, beyond an optimal point (4:1), excessive KOH (ratio 5:1) causes over-etching, leading to partial pore wall collapse and a decrease in S_BET, as observed with ELC700-2-5. More importantly, the ratio controls the pore size distribution. Lower KOH amounts favor predominantly microporous structures (e.g., ELC700-2-2 with 90.59% microporosity), while higher amounts promote the development of mesopores, reducing the microporosity percentage. Carbonization temperature plays a similar role; higher temperatures intensify the etching reactions. Raising the temperature from 650 °C to 750 °C generally increases both the BET SSA and total pore volume, yet also shifts the pore size distribution toward larger pores; at 800 °C, the micropore proportion drops notably to 26.16% for ELC800-2-4.

Carbonization time provides fine-tuning; shorter times (1h) may not allow complete pore development, while the optimal 2h yields the best-balanced structure.

The exceptional electrochemical performance exhibited by the optimized sample ELC700-2-4 (C/KOH = 4:1, T = 700°C, t = 2 h), achieving a specific capacitance of 443 F/g in a three-electrode configuration, stems directly from its optimally engineered hierarchical porous architecture.Its high S_BET of 3067 m^2/g provides an extensive interface for charge accumulation. Crucially, its pore architecture features a high volume of micropores (1.14 cm^3/g, 62.18% microporosity) interconnected by a network of mesopores (evidenced by the H4-type hysteresis loop in N_2 adsorption isotherms). Micropores, particularly those in the 0.35–0.7 nm range, are essential for high charge storage density due to the close proximity of ion centers to the pore walls, enhancing the quantum capacitance effect and allowing for very high volumetric capacitance. However, ion access to these deep micropores can be kinetically limited. This is where the co-existing mesopores (2–5 nm) become critical. These mesoporous channels function as low-resistance ionic pathways, enabling efficient and rapid transport of electrolyte ions (K^+ and OH^- in 6 M KOH) from the bulk solution to the micropore entrances, thereby significantly minimizing ionic diffusion limitations. This hierarchical design effectively decouples the ion transport pathway (through mesopores) from the charge storage zones (within micropores), resolving the classic trade-off between high capacitance (needs high S_BET from micropores) and high rate capability (needs facile ion transport through larger pores).

The electrochemical findings offer strong validation for this structure-dependent mechanism. The quasi-rectangular CV traces and isosceles-triangular GCD waveforms collectively confirm optimal EDLC performance with swift charge propagation and outstanding cycling fidelity.This is already well-paraphrased. Here is a slightly alternative version:

Impedance analysis provides additional validation: the modest and comparable equivalent series resistance (R_s ≈ 0.58 Ω) observed for the majority of samples suggests adequate inherent electronic conductivity of the carbon structure and consistent manufacturing reproducibility, whereas the interfacial charge transfer resistance demonstrates greater sample-to-sample divergence. ELC700-2-4 achieves the minimal R_ct value (0.0851 Ω) across the varying carbon-to-alkali compositions, indicative of the most favorable interfacial kinetics, which stems from its rationally designed mesoporous architecture that effectively alleviates ionic transport hindrances.The remarkable cycling durability (95.55% capacitance retention after 10,000 cycles) exhibited by the symmetric supercapacitor assembled with ELC700-2-4 originates from the robust physical and chemical stability of the carbon framework, coupled with the purely physical,non-faradaic charge storage mechanism characteristic of electric double-layer capacitors, which precludes structural deterioration typically associated with phase transformations in battery-type materials.In conclusion, the high performance of the lignin-derived porous carbon is mechanistically rooted in the KOH carbonization process that creates a hierarchical pore structure. I notice this was my own previous response being echoed back. Here is a fresh alternative paraphrase:

The strategic combination of extensive microporosity enabling high-density charge accommodation alongside an optimized mesoporous network facilitating efficient ionic transport serves as the fundamental architectural basis for realizing superior specific capacitance, excellent high-rate performance, and outstanding long-term stability. This work successfully establishes an unambiguous and implementable framework linking structural design, material characteristics, and electrochemical functionality for bio-based carbon electrodes in supercapacitor applications.Based on the comprehensive findings presented in the document, the future application prospects for the enzymatic hydrolysis lignin-based porous carbons (ELCs), particularly the optimized ELC700-2-4 material, are highly promising and span several critical areas of advanced energy storage and environmental technology. The foremost and most immediate application resides in the development of advanced, environmentally sustainable supercapacitor technologies. The material's remarkable gravimetric capacitance (443 F/g under three-electrode configuration), superior high-rate performance, and exceptional durability (95.55% capacitance preservation following 10,000 charge-discharge cycles) render it a highly viable candidate for commercial-scale electrochemical capacitor deployment.This is already well-paraphrased. Here is a slightly alternative version:

Such supercapacitor devices are ideally suited for deployment in applications necessitating rapid charge-discharge cycling and high specific power, including regenerative braking energy capture in electric and hybrid automotive platforms, frequency modulation services in modernized electrical grids, and emergency backup

power systems for essential equipment and industrial machinery. The use of biomass-derived lignin addresses the growing demand for eco-friendly and cost-effective alternatives to fossil-based carbons, aligning with global sustainability goals. Furthermore, the demonstrated energy density (8.6 W·h/kg at ~500 W/kg) of the symmetric supercapacitor, while modest, provides a foundation for further development. Future research directions may involve incorporating this lignin-derived carbon material with pseudocapacitive components (such as transition metal oxides or electroactive conducting polymers) to develop hybrid supercapacitor systems,thereby substantially enhancing the energy density while preserving the high power capability and extended cycling lifespan, potentially narrowing the performance gap between conventional supercapacitors and battery technologies.Another promising avenue for practical implementation lies in the domain of integrated energy storage architectures.The favorable electrochemical performance demonstrated by this material in aqueous KOH electrolyte indicates its immediate suitability for deployment in safe,cost-effective, and environmentally sustainable energy storage systems.Moreover, its well-defined hierarchical pore structure, proven to be tunable via the KOH carbonization parameters, is not only beneficial for ion adsorption in supercapacitors but also suggests potential in other areas requiring high-surface-area functional carbons. For instance, these lignin-derived porous carbons could be explored as efficient adsorbents for water purification (e.g., removing heavy metals or organic pollutants) or for gas separation and storage (e.g., CO_2 capture), adding another dimension to the valorization of biomass waste. The documented ability to dope the carbon with heteroatoms like N and O (evident from the elemental mapping) during the one-pot process also opens avenues for enhancing its catalytic performance, potentially applying it as a metal-free catalyst or catalyst support in various chemical reactions. From a manufacturing and scalability perspective, the process described is relatively straightforward, using a single-step carbonization of a low-cost, abundant industrial byproduct (enzyme hydrolysis lignin). This offers a compelling route for large-scale, cost-effective production of functional carbon materials, contributing to a circular bio-economy. Future research and development should focus on process intensification, life-cycle assessment to quantify the environmental benefits, and the fabrication of practical electrode devices (e.g., flexible or printed electrodes) to transition this promising laboratory-scale material into real-world applications, ultimately supporting the advancement of renewable energy infrastructure and sustainable industrial practices.

Conclusion

Drawing upon the extensive experimental investigation presented herein, the following salient conclusions regarding the synthesis and practical implementation of porous carbon materials derived from enzymatic hydrolysis lignin through KOH-mediated activation can be formulated:An optimized and scalable process for high-performance carbon material was successfully established. The study demonstrates that high-quality porous carbon can be efficiently produced in a single step from the abundant and renewable biomass waste, enzymatic hydrolysis lignin. The optimal synthesis parameters were identified as an activation temperature of 700 °C, a carbon-to-alkali (KOH) mass ratio of 4:1, and an activation time of 2 hours. Under these conditions, the resulting material (ELC700-2-4) shows an excellent combination of a high SSA (3067 m^2/g) and a well-developed hierarchical pore structure with a microporosity of 62.18%.

The prepared material exhibits outstanding electrochemical performance suitable for supercapacitor electrodes. The ELC700-2-4 sample demonstrated superior electric double-layer capacitive behavior in 6 M KOH electrolyte.In a three-electrode system, the material achieved a remarkable gravimetric capacitance of 443 F/g at a current density of 1 A/g. This is already well-paraphrased. Here is a slightly alternative version:

When assembled into a practical symmetric supercapacitor, the electrode maintained a specific capacitance of 250 F/g at 1 A/g, and showed excellent long-term stability with 95.55% of its initial capacitance retained after 10,000 consecutive galvanostatic charge–discharge cycles.The assembled device reached an energy density of 8.6 Wh/kg at a power density of 500.16 W/kg. This study provides a feasible and eco-friendly strategy for converting lignocellulosic waste into high-value energy storage materials. The study successfully establishes a direct correlation between the refinement of chemical activation parameters, the precise engineering of porous structures, and the resultant improvement in electrochemical performance characteristics. The successful conversion of low-value enzymatic hydrolysis lignin into a high-value porous carbon electrode material not only offers a promising candidate for cost-effective and environmentally friendly supercapacitors but also contributes to the development of a circular economy and the advancement of green energy storage technologies.

References

[1] ZHANG W J, GUO T Y, LIU Y H, et al. Electrocatalytic Performance of Carbon Layer and Spherical Carbon/Carbon Cloth Composites towards Hydrogen Evolution from the Direct Electrolysis of Bunsen Reaction Product [J]. Chemical Research in Chinese Universities, 2024, 40(1): 109-118.

[2] TOMO T, ALLAKHVERDIEV S I. Preface: Photosynthesis and Hydrogen Energy Research for Sustainability [J]. Photosynthesis Research, 2017, 133(1): 1-3.

[3] BI H H, HE X J, ZHANG H F, et al. N,P Co-doped Hierarchical Porous Carbon from Rapeseed Cake with Enhanced Supercapacitance [J]. Renewable Energy, 2021, 170: 188-196.

[4] CAI N, CHENG H, HAN J, et al. Porous Carbon Derived from Cashew Nut Husk Biomass Waste for High-Performance Supercapacitors [J]. Journal of Electroanalytical Chemistry, 2020, 861: 113933-1-113933-7.

[5] WATKINS D, NURUDDIN M, HOSUR M, et al. Extraction and Characterization of Lignin from Different Biomass Resources [J]. JMR&T, 2015, 4(1): 26-32.

[6] DONG Y, LIU L, WANG X Y, et al. Biomass-Derived Activated Carbon Nanoarchitectonics with Hibiscus Flowers for High-Performance Supercapacitor Electrode Applications [J]. Chemical Engineering & Technology, 2022, 45(4): 649-657.

[7] ZHANG Y, ZHAO Y P, QIU L L, et al. Insights into the KOH Activation Parameters in the Preparation of Corncob-Based Microporous Carbon for High-Performance Supercapacitors [J]. Diamond and Related Materials, 2022, 129: 109331-1-109331-12.

[8] YANG S, WANG S L, LIU X, et al. Biomass Derived Interconnected Hierarchical Micro-meso-macro-porous Carbon with Ultrahigh Capacitance for Supercapacitors [J]. Diamond and Related Materials, 2019, 147: 540-549.

[9] GENOVESE M, JIANG J H, LIAN K, et al. High Capacitive Performance of Exfoliated Biochar Nanosheets from Biomass Waste Corn Cob [J]. Journal of Materials Chemistry A, 2015, 3(6): 2903-2913.

[10] LIU F Y, GAO Y Y, ZHANG C S, et al. Highly Microporous Carbon with Nitrogen-Doping Derived from Natural Biowaste for High-Performance Flexible Solid-State Supercapacitor [J]. Journal of Colloid and Interface Science, 2019, 548: 322-332.

[11] ZHANG G L, GUAN T T, WANG N, et al. Small Mesopore Engineering of Pitch-Based Porous Carbons toward Enhanced Supercapacitor Performance [J]. Chemical Engineering Journal, 2020, 399: 125818-1-125818-9.

[12] XIE L J, SU F Y, XIE L F, et al. Effect of Pore Structure and Doping Species on Charge Storage Mechanisms in Porous Carbon-Based Supercapacitors [J]. Materials Chemistry Frontiers, 2020, 4(9): 2610-2634.

[13] SHI F Y, TONG Y, LI H S, et al. Synthesis of Oxygen/Nitrogen/Sulfur Codoped Hierarchical Porous Carbon from Enzymatically Hydrolyzed Lignin for High-Performance Supercapacitors [J]. Journal of Energy Storage, 2022, 52: 104992-1-104992-10.

[14] KLOSE M, REINHOLD R, LOGSCH F, et al. Softwood Lignin as a Sustainable Feedstock for Porous Carbons as Active Material for Supercapacitors Using an Ionic Liquid Electrolyte [J]. ACS Sustainable Chemistry & Engineering, 2017, 5(5): 4094-4102.

[15] WAN X, SHEN F, HU J G, et al. 3-D Hierarchical Porous Carbon from Oxidized Lignin by One-Step Activation for High-Performance Supercapacitor [J]. International Journal of Biological Macromolecules, 2021, 180: 51-60.

[16] SHANG M G, ZHANG J, LIU X C, et al. N,S Self-doped Hollow-Sphere Porous Carbon Derived from Puffball Spores for High Performance Supercapacitors [J]. Applied Surface Science, 2021, 542: 148697.

[17] KIM H, CHO J Y, JANG S Y, et al. Deformation-Immunized Optical Deposition of Graphene for Ultrafast Pulsed Lasers [J]. Applied Physics Letters, 2011, 98(2): 021104.

[18] ZHAO J, ZHANG W J, SHEN D K, et al. Preparation of Porous Carbon Materials from Black Liquor Lignin and Its Utilization as CO_2 Adsorbents [J]. Journal of the Energy Institute, 2023, 107: 101179-1-101179-9.

[19] YU D, MA Y S, CHEN M F, et al. KOH Activation of Wax Gourd-Derived Carbon Materials with High Porosity and Heteroatom Content for Aqueous or All-Solid-State Supercapacitors [J]. Journal of Colloid and Interface Science, 2019, 537: 569-578.

[20] FU X Y, LIU L, YU Y F, et al. Hollow Carbon Spheres/Hollow Carbon Nanorods Composites as Electrode Materials for Supercapacitor [J]. Journal of the Taiwan Institute of Chemical Engineers, 2019, 101: 244-250.

[21] NG S W L, YILMAZ G, ONG W L, et al. One-Step Activation towards Spontaneous Etching of Hollow and Hierarchical Porous Carbon Nanospheres for Enhanced Pollutant Adsorption and Energy Storage [J]. Applied Catalysis B: Environmental, 2018, 220: 533-541.

[22] CHEN H, LIU D, SHEN Z H, et al. Functional Biomass Carbons with Hierarchical Porous Structure for

Supercapacitor Electrode Materials [J]. Electrochimica Acta, 2015, 180: 241-251.
[23] WU Y, CAO J P, ZHAN X Y, et al. Preparation of Porous Carbons by Hydrothermal Carbonization and KOH Activation of Lignite and Their Performance for Electric Double Layer Capacitor [J]. Electrochimica Acta, 2017, 252: 397-407.
[24] CHENG Y L, ZHANG Q L, FANG C Q, et al. Synthesis of N-Doped Porous Carbon Materials Derived from Waste Cellulose Acetate Fiber via Urea Activation and Its Potential Application in Supercapacitors [J]. Journal of the Electrochemical Society, 2019, 166(6): A1231-A1238.
[25] GOPALAKRISHNAN A, BADHULIKA S. Ultrathin Graphene-Like 2D Porous Carbon Nanosheets and Its Excellent Capacitance Retention for Supercapacitor [J]. Journal of Industrial and Engineering Chemistry, 2018, 68: 257-266.
[26] HE Z N, ZHANG G X, CHEN Y M, et al. The Effect of Activation Methods on the Electrochemical Performance of Ordered Mesoporous Carbon for Supercapacitor Applications [J]. Journal of Materials Science, 2017, 52(5): 2422-2434.
[27] YANG J Y, CEN W F, TIAN Z A. Effect of Biaxial Strain on the Electronic Structure and Optical Performance of Two-Dimensional [J]. Physica Scripta, 2024, 99(8): 085927-1-085927-13.
[28] ZHANG H F, HE X J, WEI F, et al. Moss-Covered Rock-Like Hybrid Porous Carbons with Enhanced Electrochemical Performance [J]. ACS Sustainable Chemistry & Engineering, 2020, 8(8): 3065-3071.
[29] ZHANG J Y, XIA C, WANG H F, et al. Recent Advances in Electrocatalytic Oxygen Reduction for On-Site Hydrogen Peroxide Synthesis in Acidic Media [J]. Journal of Energy Chemistry, 2022, 67: 432-450.
[30] ZHANG Y L, TANG Z S. Porous Carbon Derived from Herbal Plant Waste for Supercapacitor Electrodes with Ultrahigh Specific Capacitance and Excellent Energy Density [J]. Waste Management, 2020, 106: 250-260.